Jomard Publishing

Advances in Biology & Earth Sciences., V.1, N.1, 2016, pp.89-106

DIFFUSION KURTOSIS IMAGING METRICS AS NON-INVASIVE BIOMARKERS IN BRAIN GLIOMA GRADING

Igor Pronin[*,1] A. Tonoyan[1], F. Grinberg[2,3], E. Farrher[2], I. Maximov[2], L. Shishkina[1], N. Zakharova[1], E. Shults[1], N. Shah[2,3], A. Potapov[1]

[*]***Academician of Russian Academy of Sciences***
[1]Burdenko Neurosurgery Institute, 125047, Moscow, Russia
[2]Institute of Neuroscience and Medicine - 4, Forschungszentrum Juelich GmbH, 52425, Juelich, Germany
[3]Department of Neurology, Faculty of Medicine, RWTH Aachen University, 52074 Aachen, Germany
e-mail: eshults@nsi.ru

Abstract: DKI parameters exhibit higher sensitivity and specificity in discriminating between various glioma's grades than the DTI parameters, exhibiting higher sensitivity to microstructural changes occurring during malignancy progression. DKI provides valuable non-invasive biomarkers in assessment of gliomas and has been shown to be a useful supplement to other modern neuroimaging methods. This is the first time when kurtosis anisotropy (KA) was applied in glioma grade differentiation.

Keywords: glioma, diffusion, tumor, kurtosis, WHO grade.

Abbreviations

MD – mean diffusivity
AD – axial diffusivity
RD – radial diffusivity
FA – fractional anisotropy
RA – relative anisotropy
MK – mean kurtosis
AK – axial kurtosis
RK – radial kurtosis
KA – kurtosis anisotropy
LGG – low grade gliomas (including grades I and II)
HGG – high grade gliomas (including grades III and IV)
CNAWM – contralateral normal appearing white matter
NAWM – normal appearing white matter
ROI – region of interest
DKI – diffusion kurtosis imaging
DTI – diffusion tensor imaging
WI – weighted images
WHO – World Health Organisation
CNS – central nervous system

1. Introduction

Gliomas are one of the most frequently found types of human brain tumours and comprise about 50% of all primary brain tumours in adults. Gliomas cover a broad range of lesions of different aetiology and malignancy. The World Health Organisation (WHO) classification of tumours in the central nervous system (CNS) allows one to subdivide the large amount of CNS tumours into 4 groups according to their malignancy degree [1] and, based on that, forecast their biological activity. The WHO grade of the tumour as well as its location and lesion features visualised by neuroimaging, the age of the patient, his neurological status, radicality of surgical resection and proliferation indices of the tumour are all extremely important in predicting the outcome of surgery, chemotherapy, radiation treatment, and for a survival rate [1]. Glioma grading is mainly based on histological and immunohistochemical features of the tumour such as nuclear atypia, vessel endothelial cell proliferation, mitotic activity and the presence of necrosis [1]. The histopathological examination of tissue requires invasive manipulations, for example, a surgery or biopsy with concomitant risks. Therefore, it is important to analyse and apply new methods in frame of the preoperative assessment of the tumour grade in order to prevent avoidable invasive interventions.

Diffusion tensor imaging (DTI) has proven to be a valuable tool in glioma grading. However, reports on sensitivity and specificity of diffusion scalar metrics in the detection of cellular changes related to the malignant progression obtained by different authors have been controversial [2-7].DTI is based on the simplified assumption of the Gaussian diffusion of water molecules in brain tissue, which appears valid only in the low range of diffusion weightings (so called *b*-values), i.e., $b< 1000$ s/mm^2. Water diffusion in biological tissue is restricted and hindered due to the presence of different compartments, cell membranes, intracellular organelles, axons, etc., giving rise to deviations from the Gaussian diffusion at higher *b*-values. Diffusion kurtosis imaging (DKI) is a novel modality in diffusion MRI which allows one to assess the non-Gaussianity of molecular diffusion at higher *b*-values in biological tissue [8].

Only a few works investigating the use of DKI in the grading of brain gliomas have been published so far[4, 6, 9, 10]. In general, an important finding of these works was that diffusion kurtosis parameters provide very promising novel biomarkers for differentiation between the low and high grade gliomas. However, these innovative studies also suffered form certain methodological limitations. Firstly, the size of patient groups used in the analysis was relatively small (about 28-35 subjects [4, 6, 9] including both low and high tumour grades). Therefore, the reported findings are to be confirmed by the independent studies using larger subject groups for higher statistical reliability. Secondly, most of the attention in the analysis was given to the mean kurtosis (MK) [4, 6, 9], whereas other DKI scalar metrics, such as axial (AK) and radial (RK) diffusional kurtoses, potentially useful in assessment of microstructural changes, have been additionally considered in one work [6] only. Thirdly, a more detailed differentiation between glioma grades have been studied with very low group sizes, such as 5 grade II

astrocytomas, 13 grade III astrocytomas, and 16 grade IV glioblastomas [4], while other authors [6, 9] have roughly compared low and high grade gliomas.

The goal of our work was to study the benefits of DKI in assessment of glioma malignancy using the large group of patients (n=84) and with a significantly improved statistical power of the study design in comparison to previous works. We were also able to more reliably differentiate between gliomas-III and gliomas-IV cases within the same HGG group, as well as between gliomas-II and gliomas-III. We therefore could estimate advantages of novel DKI biomarkers in assessing microstructural changes that underlie the tumour malignancy progression.

Several DKI metrics used in this work, namely, AK, RK, and kurtosis anisotropy (KA), were applied to discriminate beween LGG and gliomas-III, and between gliomas-III and gliomas-IV for the first time. In difference to the previous works [4, 6, 9], we also took a more rigorous approach to specify the regions-of-interest (ROIs): only glioma regions with the maximal MK were included in the analysis assuming that these regions reveal the highest malignancy. We believe that this is a more advanced approach better corresponding to the pathomorphology of the tumour and making the statistical analysis less vulnerable to tumour's spatial heterogeneity.

2. Methods

The study was approved by the institutional ethic committee. Written, informed consent was obtained from all patients. In general, 84 patients with supratentorial gliomas were enrolled in this study. All patients have undergone imaging at the Burdenko Neurosurgery Institute where they have later been treated. All gliomas were newly diagnosed, i.e. prior to any radiation, surgery or chemotherapy. Patients with other oncologic history were excluded from the study. All patients underwent tumour removal in 1-2 weeks after undergoing DKI. The diagnoses of glioma and tumour grade were confirmed at histology and immunohistochemical examination in all cases by a neuropathomorphologist (X.X.X. with 25 years of experiance).

According to the generally accepted approach [1], HGG include grade III (gliomas-III) and grade IV gliomas (gliomas-IV) and LGG include grade I (gliomas-I) and grade II gliomas (gliomas-II). This study included 49 patients with HGG (29 gliomas-IV and 20 gliomas-III) and 35 patients with LGG (32 gliomas-II and 3 gliomas-I). The group of patients with gliomas-IV consisted of 28 patients with glioblastomas and one patient with gliosarcoma. The group of patients with gliomas-III consisted of 15 patients with anaplastic astrocytomas, one patient with anaplastic oligodendroglioma and 4 patients with anaplastic oligoastrocytoma. The group of patients with gliomas-II consisted of 23 patients with diffuse fibrillaryastrocytomas, 7 patients with oligoastrocytomas, and 2 patients with oligodendrogliomas. The group of patients with gliomas-I consisted of 1 patient with papillary glioneuronal tumour, 1 patient with subependimal giant cell astrocytoma and one patient with dysembryoplasticneuroepithelialtumour.

This study included 47 male and 37 female patients in the age range from 18 to 59 years old (average age for HGG - 43,8±14,7, for LGG - 37,7±9.6 years old).

All patients underwent DKI with a 3T MRI scanner using a diffusion weighted spin-echo echo-planar imaging sequence (DW-SE-EPI). Protocol parameters included: three *b*-values (0, 1000 and 2500 s/mm^2) and 60 diffusion gradient directions for each non-zero *b*-value; repetition time, TR = 10000 ms; echo-time, TE = 103.4 ms; field-of-view, FOV = 240×240 mm^2; matrix-size 80×80 with interpolation to 256×256; slice thickness = 3 mm; intersection gap = 0 mm; number of slices = 32; number of excitations, NEX = 1. DKI was acquired in the axial plane, with an acquisition time of 22 minutes. Additionally, anatomic reference images consisting of axial T2-weighted images (TR = 4300 ms; TE = 85 ms; turbo factor = 21; FOV = 240×240 mm; matrix-size = 512×512; slice thickness = 3 mm; intersection gap = 0 mm; NEX = 2); T2-FLAIR-weighted images (TR = 9500 ms; TE = 120 ms; inversion time, TI = 2250 ms; FOV = 240×240 mm; matrix = 352×325; slice thickness = 5 mm; intersection gap = 0 mm; NEX = 1) were acquired before the gadolinium (Gd) contrast agent administration and T1-weighted images (TR = 875 ms; TE = 85 ms; FOV = 240×240 mm; matrix-size = 384×384, slice thickness = 3 mm, intersection gap = 0 m; NEX = 2) were acquired before and after Gd contrast agent administration (0.1 mmol/kg).

Prior to the assessment of the DKI metrics, diffusion data were corrected for eddy-current distortions and head motion using the FSL toolkit [11] and the diffusion gradient directions were corrected accordingly using in-house Matlab scripts [12] (Matlab, The MathWorks, Natick, MA, USA). Bias due to background noise was reduced using the power-images method [13, 14]. The following DTI/DKI parameters were evaluated as described elsewhere [15] using the ExploreDTI toolkit [16]: mean diffusivity (MD), axial diffusivity (AD), radial diffusivity (RD), fractional anisotropy (FA), relative anisotropy (RA), mean kurtosis (MK), axial kurtosis (AK), radial kurtosis (RK), kurtosis anisotropy (KA). In order to avoid outliers the REKINDL approach was used [17].

Regions of interest (ROI) were manually drawn by two trained neuroradiologists (A.S.T. with 5 years of experience and I.N.P., with 29 years of experience) on the MK maps around the solid tumour parts (Figs. 1-3) and the contralateral normal-appearing white matter (CNAWM) (Fig. 2d) using ITK-SNAP [18] (http://www.itksnap.orghttp://www.itksnap.org/pmwiki/pmwiki.php) in accordance with anatomic reference MR images. Afterward, the ROIs were automatically mapped to other DKI metrics. Cystic, hemorragic and necrotic tumour components, peritumoral brain oedema were excluded from the ROIs.

An important issue to take into account is that most of the gliomas become frequently more malignant along time [19]. Moreover, glial tumours often have heterogeneous structure, including different malignant grade areas simultaneously. According to pathomorphology, the most malignant region of the glioma determines its grade, while the tumor may include regions of lower malignancy. As shown by several authors [4, 6], MK increases significantly with higher glioma grade. Here, we assumed that the glioma regions with maximal MK values correspond to the most malignant regions of the tumour. Therefore, in order to

provide higher reliability of our analysis, the ROIs in MK maps included the brightest regions in glioma areas (Figs. 1-3). Areas of tumour infiltration into the brain tissue were excluded from the ROIs, since brain tissue remainders in a tumor can erroneously increase tumour kurtosis and anisotropy values and decrease diffusivity (Fig.1).

In order to reduce inter-subject variations [20-23], diffusion metrics from tumour regions were normalized with respect to the corresponding parameters measured in the CNAWM. As an example, the normalized MK values were evaluated as MK (tumour) / MK (CNAWM). The same procedure was used for all other parameters (Fig. 2) [24, 25].

Absolute and normalized DTI/DKI parameters were compared between HGG and LGG, LGG and gliomas-III, gliomas-III and gliomas-IV using the Mann-Whitney test. The statistical significance threshold was $p< 0.05$. Receiver operating characteristic (ROC) curves were generated for all absolute and normalized diffusion parameters to assess the area under curve (AUC) of the ROC and to determine the optimum parameter threshold in each group.

3. Results

The results of the comparison of DTI/DKI parameters between HGG and LGG are shown in Table 1. All absolute and normalized diffusion parameters, except for absolute KA, FA, RA and normalized FA and RA, significantly differ between HGG and LGG ($p < 0.05$). AUC of the ROC was the highest for the normalized MK values (0.956). The highest sensitivity and specificity were found for the normalized MK (88.57% and 87.76%, respectively).

The results of the comparison of DTI/DKI parameters between gliomas-III and gliomas-IV are shown in Table 2. All absolute and normalized diffusion parameters, except for FA and RA, differ significantly between gliomas-III and gliomas-IV ($p < 0.05$). AUC of the ROC was the highest for normalized MK (0.946). The highest sensitivity and specificity were found for absolute MK (90.00 and 89.66%, respectively) and normalized MK (90.00 and 89.66%, respectively).

The results of the comparison of DTI/DKI parameters between LGG and gliomas-III are shown in Table 3. The absolute values of MK, AK, RK and the normalized values of MK, AK, RK, and RD differ significantly between LGG and gliomas-III ($p <0.05$). AUC of the ROC was the highest for the normalized values of MK (0.896). The highest sensitivity and specificity were found for normalized values of MK (80.00% and 80.00%, respectively).

4. Discussion

There is a large number of published works regarding the application of DTI in glioma grading [2, 4-6, 9, 26-43]. It is already well established that MD decreases with higher glioma grade [4, 6, 9, 26, 29, 30, 32, 35, 39]. In many studies it was also shown that both, absolute [9, 26] and normalized [6] values of MD are significantly lower in HGG than in LGG. Additionally, it was found that the absolute and normalized MD values differ significantly between anaplastic

astrocytomas and glioblastomas [4]. A correlation between minimal MD and glioma malignancy was also observed [29, 30, 32, 35, 39], i.e., minimal MD values were significantly lower in HGG than in LGG [30, 32, 35], in gliomas-IV than in gliomas-III [29, 39], in gliomas-III than in gliomas-II [30, 39] and in HGG than in gliomas-II [30, 39]. Minimal normalized MD values have been shown to differ significantly between gliomas-II and gliomas-III, gliomas-II and gliomas-IV, gliomas-II and HGG [39], LGG and HGG [30, 35].

In spite of a large amount of works, one can still find some controversy in the literature regarding the correlation between MD and glioma malignancy. Several authors suggested that MD is not consistently helpful in differentiating among glioma grades [28, 31, 34, 37, 43]. It has been shown that differences in MD [5, 6, 36-38] and minimal MD [36] between HGG and LGG were non-significant. Other authors found that minimal MD is not suitable for differentiating between anaplastic astrocytoma and glioblastoma [29, 32].

Some other works [39, 42] made use of AD and RD in glioma grading. The absolute values of minimal AD and RD and normalized values of minimal RD differed significantly between gliomas-II and gliomas-III, gliomas-II and gliomas-IV, gliomas-II and HGG [39], while the normalized minimal AD values differed significantly between gliomas-II, gliomas-III and gliomas-IV [39]. Also AD and RD differed significantly between HGG and LGG [42].

Furthermore, it has been demonstrated that FA differs significantly between HGG and LGG [26, 27, 31, 33, 36]. Absolute and normalized values of minimal FA were significantly lower in gliomas-IV than in gliomas-III [39], while maximal FA was significantly lower in LGG than in HGG [36]. It has been shown that if the density of the tumour cells is the same in both contrast enhancing and nonenhancing regions of gliomas, FA values are higher in the nonenhancing area due to the remaining white matter fibres [33]. Some authors believe that FA significantly differs between gliomas-II and gliomas-III only in the peripheral tumour region, while in the central tumour region FA values are almost the same. This is due to a complete destruction of neural fibres in the centre of both lesions [2]. However, analysis based on the correlation of FA with glioma malignancy is also ambiguous. Some authors did not find any significant differences of FA values between glioma grades [2, 4-6, 27, 33, 38-40, 42]. This might be due to the fact that the most of HGG arise from LGG [44].

In general, disagreements among the published reports can rise up, among others, due to the differences in the data acquisition protocols and post-processing methods [25]. Another essential affecting factor is the delineation of ROIs used for evaluation of the diffusion parameters.

Regarding the use of DKI parameters in grading of brain gliomas, only a few studies have been published so far [4, 6, 9, 10]. It was reported that the absolute MK, AK, RK values and the normalized MK and RK values were significantly higher in the case of HGG than in LGG, while the normalized AK values did not differ significantly between these two groups [6]. According to other authors, the absolute and normalized MK values differed significantly between grade-II, grade-III and grade-IV gliomas [4].

It is well known that gliomas tend to progress to a higher malignancy grade with time [1]. This is often the reason of their heterogeneity given that the same tumour may have regions with different malignancy grades [19]. According to pathomorphology [1], the true malignancy grade of a tumour is determined via its most malignant regions. That is why in the present study, in contrast to previous publications [4, 6, 9, 10], we assumed that the group comparisons based on the most malignant glioma regions should be more efficient. We based our approach on the assumption that the highest MK values correspond to the most malignant tumour areas [4, 6, 9, 10]. Therefore, our ROIs included only the tumour areas with the highest MK. Cystic, hemorragic and necrotic tumour components, peritumoraledema, tumour regions with brain tissue remainders were excluded from the ROIs. Diffusion in cystic and necrotic tumour components is close to isotropic Gaussian. It is characterised by low diffusional kurtosis (mean, axial and radial) and anisotropy (kurtosis, fractional and relative), and high diffusivity (mean, axial and radial). Peritumoral oedema and tumour regions containing remainders of brain white matter also exhibit different diffusion and anisotropy characteristics in comparison to the central solid glioma areas due to the presence of neural fibres [2, 33].

Our results demonstrated consistency with previously published studies and demonstrated an increase of the absolute and normalized MK, AK, RK, KA, FA and RA values, and a decrease of the absolute and normalized MD, AD and RD values with higher malignancy grade. The increase in kurtosis metrics (MK, AK and RK) and the decrease in diffusion metrics (MD, AD and RD) with higher glioma grade is supposed to be due to the increase of the tumour cell density and the decrease of the cell size accompanied by the, decrease of the intercellular space and the increase of endothelial proliferation, i.e., the factors that restrict and hinder molecular propagation. In general, gliomas with isotropically homogenous distribution of cell density tend to exhibit low anisotropy values (KA, FA and RA) compared to white matter, which has high anisotropy due to the coherent alignment of neural fibres. However, KA, FA, and RA increase with higher glioma grade, which could be explained by the decrease of the extracellular fluid volume and appearance of diffusion directionality in the extracellular space. A comparison of KA, FA and RA with other diffusion parameters and anatomic T1- and T2-weighted images revealed remainders of white matter in the investigated gliomas (Fig. 1). So that the anisotropy alone is not an objective parameter to grade the glioma malignancy, because the remainder of a small amount of white matter will affect FA, RA and KA regardless of the tumor malignancy grade.

Our results demonstrate that diffusion kurtosis parameters (MK, AK and RK) are able to differentiate LGG from HGG, gliomas-III from gliomas-IV, LGG form gliomas-III with higher sensitivity and specificity than diffusion tensor parameters (MD, AD and RD). This is due to the fact that diffusion kurtosis metrics take into account the non-Gaussian molecular diffusion in biological tissues and thus better capture its microstructural complexity, in particular, the changes associated with glioma malignancy. According to the results of our work, normalization of diffusion metrics in tumours with respect to CNAWM improves

the differentiation between glioma grades, in consistency with previous studies [4, 6].

More than 90% of glioblastomas are primary in origin [19]. Their solid component microstructure is quite homogeneous and significantly differentiates from gliomas-III. However, most of the gliomas-III form as a consequence of focal anaplasia of gliomas-II [19]. These features suggest that the similarity between histological microstructure of gliomas-II and gliomas-III is higher than between gliomas-III and gliomas-IV. We believe that this is the reason of higher sensitivity and specificity of diffusion parameters in differentiating between gliomas-III and gliomas-IV, than in differentiating between LGG and gliomas-III.

DKI requires the acquisition of at least two nonzero *b*-values and at least 15 diffusion gradient directions. Therefore the acquisition time is longer compared with DTI that requires at least only one nonzero *b*-value and only 6 gradient directions [45, 46]. However, due to progress in hardware and software development during the last years, DKI became a clinically feasible method. DKI allows acquiring both the diffusion tensor and the diffusion kurtosis parameters during the same scanning session. Moreover, DKI provides *b* value–independent and more accurate diffusion tensor parameters (MD, AD, RD, FA and RA) compared with DTI [47, 48].

The general limitation of grading tumours using non-invasive imaging methods is that the ROIs used to delineate the tumour areas do not necessarily coincide with the portions of the tumour sent to pathomorphological examination after surgery. This is a source of hardly avoidable discrepancies between the imaging methods and histology. However, since grading the tumours during the pathomorphological examination is performed according to the most malignant portions of the exercised tissue, we believe that the advanced approach exploited in our work, i.e. delineating the ROIs based on the highest diffusion kurtosis, provides the promising means to improve the correspondence between the both methods.

5. Conclusion

In this study we demonstrate significant differences in diffusion kurtosis and diffusion tensor metrics between LGG and gliomas-III, gliomas-III and gliomas-IV, LGG and HGG. Diffusion kurtosis parameters allow one to distinguish between the grades of different groups of gliomas with higher sensitivity and specificity than diffusion tensor parameters. In particular, kurtosis metrics have higher sensitivity for the detection of microstructural changes occurring during tumour anaplasia. DKI technique provides a number of novel non-invasive biomarkers in grading brain gliomas. It is therefore a useful complimentary method in modern neuroimaging and tumour treatment.

Acknowledgement. Burdenko Neurosurgery Institute gratefully acknowledges a support by the Russian Scientific Foundation (RSF) grant № 14-15-00197. IIM thanks DFG (Deutsche Forschungsgemeinschaft) grant (SU 192/32-1) for a partial support.

Pathology

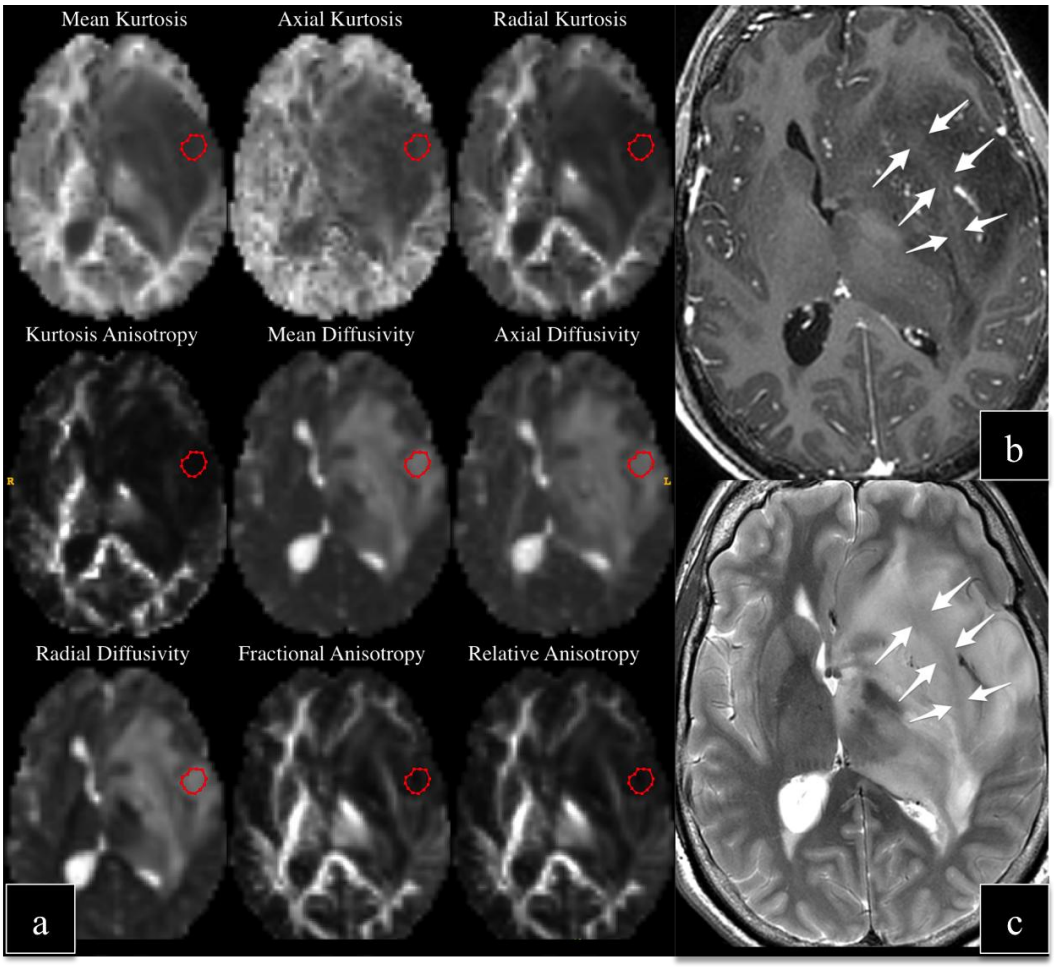

Fig. 1. Diffuse astrocytoma WHO grade-II, without signal enhancement after Gd administration: a) DKI scalar metrics, b) T1-weighted image with Gd-enhancement, c) T2-weighted image. The ROI includes the most homogeneous area of the tumour (a). Tumour areas with remainders of brain tissue (see arrows on T1-w (b) and T2-w (c)) are excluded from the ROI because they can contribute to the artificial increase of the kurtosis (MK, RK and AK) and anisotropy values (FA, RA and KA) and the decrease of diffusivity values (MD, RD and AD) (a).

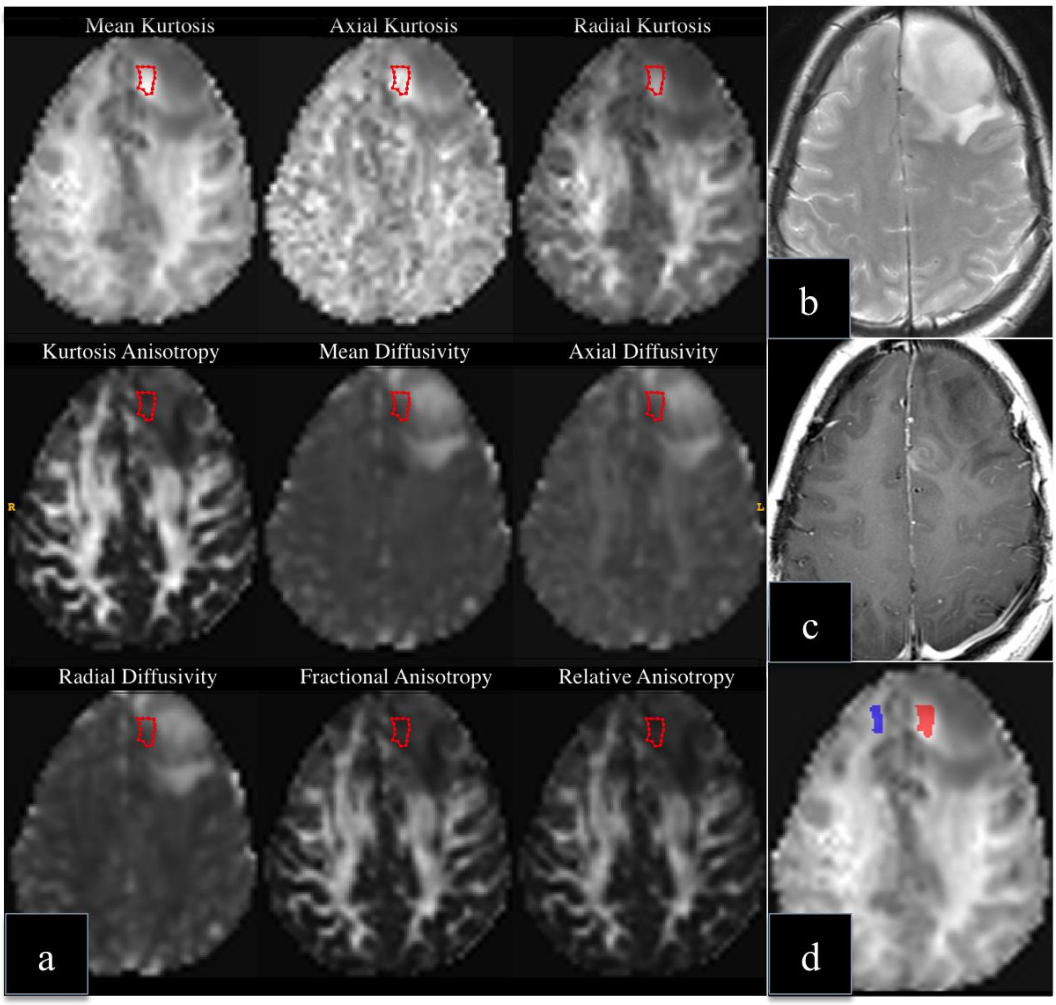

Fig. 2. Anaplastic astrocytoma WHO grade-III of the frontal lobe: a) DKI scalar metrics, b) T2-weighted image, c) T1-weighted image with Gd-enhancement, d) the ROIs around the tumour and the contralateral normal appearing white matter on MK maps. Local mild tumour-enhancement is shown (see the arrow in c). The ROI includes the tumour area with the maximal MK values which is supposed to correspond to the maximal malignancy, although it does not fully correspond to the signal enhancement after Gd administration (a).

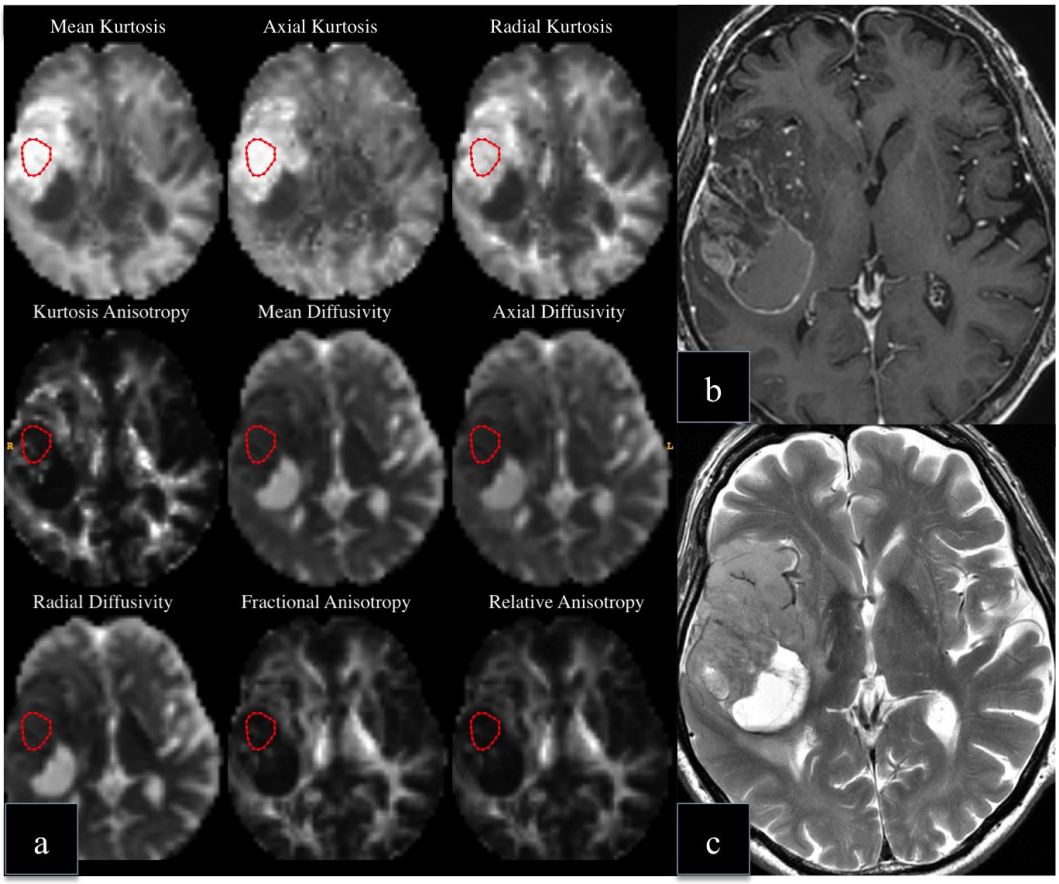

Fig. 3. Glioblastoma WHO grade-IV: a) DKI scalar metrics, b) T1-weighted image with Gd-enhancement, c) T2-weighted image. The ROI includes a solid fraction of the tumour with maximal MK supposed to correspond to the maximal malignancy (a). Peritumoral oedema and necrosis are excluded from the ROI (a).

Table 1. Differentiation between HGG and LGG.

Diffusion parameters	*p*-threshold	AUC ROC	Sensitivity (%)	Specificity (%)	Optimal threshold	HGG		LGG	
						Mean	SD	Mean	SD
MK	<0,001	0,925	82,86	83,67	0,479	0,794	0,257	0,467	0,141
AK	<0,001	0,910	82,86	81,63	0,461	0,692	0,192	0,441	0,127
RK	<0,001	0,916	85,71	85,71	0,489	0,839	0,299	0,485	0,156
KA	>0,05	-	-	-	-	0,068	0,041	0,049	0,025
MD (10^{-2} mm^2/s)	<0,001	0,817	74,29	75,51	0,156	0,127	0,047	0,178	0,038
AD (10^{-2} mm^2/s)	<0,001	0,818	77,14	75,51	0,165	0,141	0,052	0,198	0,040
RD (10^{-2} mm^2/s)	<0,001	0,818	74,29	75,51	0,144	0,120	0,045	0,168	0,037
FA	>0,05	-	-	-	-	0,113	0,049	0,110	0,050
RA	>0,05	-	-	-	-	0,066	0,029	0,064	0,030
nMK	<0,001	0,956	88,57	87,76	0,505	0,885	0,266	0,494	0,139
nAK	<0,001	0,913	82,86	81,63	0,760	1,094	0,320	0,692	0,189
nRK	<0,001	0,950	85,71	85,71	0,410	0,758	0,270	0,396	0,126
nKA	<0,005	0,739	65,52	64,87	0,173	0,340	0,244	0,202	0,109
nMD	<0,001	0,852	80,00	79,59	1,489	1,210	0,427	1,806	0,391
nAD	<0,001	0,813	74,29	75,51	1,173	1,004	0,351	1,432	0,327
nRD	<0,001	0,861	80,00	79,59	1,800	1,394	0,529	2,157	0,497
nFA	>0,05	-	-	-	-	0,390	0,211	0,310	0,144
nRA	>0,05	-	-	-	-	0,379	0,213	0,295	0,142

Table 2. Differentiation between gliomas-III and gliomas-IV.

Diffusion parame-ters	*p*-thre-shold	AUC ROC	Sensi-tivity (%)	Speci-ficity(%)	Opti-mal thre-shold	Gliomas-III		Gliomas-IV	
						Mean	SD	Mean	SD
MK	<0,001	0,914	90,00	89,66	0,773	0,580	0,215	0,941	0,165
AK	<0,001	0,903	85,00	86,21	0,693	0,538	0,171	0,799	0,121
RK	<0,001	0,903	85,00	86,21	0,802	0,602	0,231	1,003	0,220
KA	<0,001	0,792	71,43	73,91	0,053	0,045	0,024	0,083	0,043
MD (10^{-2} mm^2/s)	<0,001	0,840	75,00	75,86	0,117	0,163	0,051	0,102	0,021
AD (10^{-2} mm^2/s)	<0,001	0,864	80,00	79,31	0,130	0,182	0,056	0,113	0,022
RD (10^{-2} mm^2/s)	<0,001	0,829	70,00	72,41	0,109	0,154	0,050	0,096	0,020
FA	>0,7	-	-	-	-	0,114	0,051	0,112	0,048
RA	>0,7	-	-	-	-	0,067	0,030	0,066	0,029
nMK	<0,001	0,946	90,00	89,66	0,831	0,650	0,193	1,048	0,170
nAK	<0,001	0,903	85,00	86,21	1,047	0,857	0,264	1,257	0,245
nRK	<0,001	0,900	85,00	82,76	0,714	0,530	0,158	0,915	0,212
nKA	<0,001	0,792	71,43	73,91	0,236	0,195	0,078	0,435	0,269
nMD	<0,001	0,840	75,00	75,86	1,181	1,543	0,450	0,981	0,206
nAD	<0,001	0,864	80,00	79,31	0,944	1,279	0,374	0,816	0,161
nRD	<0,001	0,829	70,00	72,41	1,304	1,780	0,563	1,129	0,293
nFA	>0,3	-	-	-	-	0,379	0,214	0,399	0,213
nRA	>0,3	-	-	-	-	0,366	0,216	0,388	0,214

Table 3. Differentiation between LGG and gliomas-III.

Diffusion parameters	*p*-threshold	AUC ROC	Sensitivity(%)	Specificity(%)	Optimal threshold	Gliomas-III		LGG	
						Mean	SD	Mean	SD
MK	0,03	0,807	68,57	70,00	0,428	0,580	0,215	0,467	0,141
AK	0,02	0,801	74,29	75,00	0,418	0,538	0,171	0,441	0,127
RK	<0,05	0,811	68,57	70,00	0,438	0,602	0,231	0,485	0,156
KA	>0,1	-	-	-	-	0,045	0,024	0,049	0,025
MD (10^{-2} mm^2/s)	>0,1	-	-	-	-	0,163	0,051	0,178	0,038
AD (10^{-2} mm^2/s)	>0,1	-	-	-	-	0,182	0,056	0,198	0,040
RD (10^{-2} mm^2/s)	>0,1	-	-	-	-	0,154	0,050	0,168	0,037
FA	>0,1	-	-	-	-	0,114	0,051	0,110	0,050
RA	>0,1	-	-	-	-	0,067	0,030	0,064	0,030
nMK	<0,001	0,896	80,00	80,00	0,478	0,650	0,193	0,494	0,139
nAK	0,01	0,761	71,43	70,00	0,689	0,857	0,264	0,692	0,189
nRK	0,002	0,884	77,14	75,00	0,384	0,530	0,158	0,396	0,126
nKA	>0,1	-	-	-	-	0,195	0,078	0,202	0,109
nMD	>0,05	-	-	-	-	1,543	0,450	1,806	0,391
nAD	>0,1	-	-	-	-	1,279	0,374	1,432	0,327
nRD	0,02	0,703	65,71	65,00	1,997	1,780	0,563	2,157	0,497
nFA	>0,05	-	-	-	-	0,379	0,214	0,310	0,144
nRA	>0,1	-	-	-	-	0,366	0,216	0,295	0,142

References

1. Louis D.N., Ohgaki H., Wiestler O.D. et al., The 2016 WHO classification of tumours of the central nervous system: a summery, Acta Neuropathol, 131, 2016, pp.803-820.
2. Goebell E., Paustenbach S., Vaeterlein O. et al., Low-grade and anaplastic gliomas: differences in architecture evaluated with diffusion-tensor MR imaging, Radiology, Vol.239, No.1, 2006, pp.217-222.
3. Lam W.W., Poon W.S., Metreweli C., Diffusion MR imaging in glioma: does it have any role in the pre-operation determination of grading of glioma? Clinical Radiology,Vol.57, No.3,2002, pp.219-225.
4. Raab P., Hattingen E., Franz K., Zanella F.E., Lanfermann H., Cerebral gliomas: diffusional kurtosis imaging analysis of microstructural differences, Radiology, Vol.254, No.3,2010, pp.876-881.
5. Tropine A., Vucurevic G., Delani P. et al., Contribution of diffusion tensor imaging to delineation of gliomas and glioblastomas, Journal of Magnetic Resonance Imaging: JMRI, Vol.20, No.6,2004, pp.905-912.
6. Van Cauter S., Veraart J., Sijbers J. et al.,Gliomas: diffusion kurtosis MR imaging in grading, Radiology,Vol.263, No.2, 2012, pp.492-501.
7. Zonari P., Baraldi P., Crisi G., Multimodal MRI in the characterization of glial neoplasms: the combined role of single-voxel MR spectroscopy, diffusion imaging and echo-planar perfusion imaging, Neuroradiology, Vol.49, No.10, 2007, pp.795-803.
8. Pott L.M., Budde A.O., Murray W.B., A proposed classification of simulators, Middle East J. Anaesthesiol., Vol.20, No.2, 2009, pp.179-185.
9. Van Cauter S., De Keyzer F., Sima D.M. et al., Integrating diffusion kurtosis imaging, dynamic susceptibility-weighted contrast-enhanced MRI, and short echo time chemical shift imaging for grading gliomas, Neuro Oncol.,Vol.16, No.7, 2014, pp.1010-1021.
10. Tonoyan A.S., Pronin I., Pitskhelauri D. et al., Diffusion kurtosis imaging in diagnostics of brain glioma malignancy, Medical Visualisation 1, 2015, pp.7-18.
11. Johansen-Berg H., Behrens T.E., Robson M.D. et al., Changes in connectivity profiles define functionally distinct regions in human medial frontal cortex, Proceedings of the National Academy of Sciences of the United States of America,Vol.101, No.36, 2004, pp.13335-13340.
12. Leemans A., Jones D.K., The B-matrix must be rotated when correcting for subject motion in DTI data, Magnetic Resonance in Medicine: Official Journal of the Society of Magnetic Resonance in Medicine / Society of Magnetic Resonance in Medicine, Vol.61, No.6, 2009, pp.1336-1349.
13. McGibney G., Smith M.R., An unbiased signal-to-noise ratio measure for magnetic resonance images, Med. Phys., Vol.20, No.4,1993, pp.1077-1078.
14. Miller A.J, Joseph P.M., The use of power images to perform quantitative analysis on low SNR MR images, Magnetic Resonance Imaging, Vol.11, No.7, 1993, pp.1051-1056.

15. Jensen J.H., Helpern J.A., MRI quantification of non-Gaussian water diffusion by kurtosis analysis, NMR in Biomedicine, Vol.23, No.7, 2010, pp.698-710.
16. Leemans A.J.B., Sijbers J., Jones D.K., ExploreDTI: A graphical toolbox for processing, analyzing, and visualizing diffusion MR data, Proceedings of the 17th Scientific Meeting, International Society for Magnetic Resonance in Medicine, 2009.
http://www.exploredti.com/ref/ExploreDTI_ISMRM_2009.pdf.
17. Tax C.M., Otte W.M., Viergever M.A., Dijkhuizen R.M., Leemans A., REKINDLE: robust extraction of kurtosis INDices with linear estimation. Magnetic Resonance in Medicine: Official Journal of the Society of Magnetic Resonance in Medicine / Society of Magnetic Resonance in Medicine, Vol.73, No.2, 2015, pp.794-808.
18. Yushkevich P.A., Piven J., Hazlett H.C. et al., User-guided 3D active contour segmentation of anatomical structures: significantly improved efficiency and reliability, NeuroImage, Vol.31, No.3, 2006, pp.1116-1128.
19. Kleihues P., Ohgaki H., Primary and secondary glioblastomas: from concept to clinical diagnosis, Neuro-Oncology, Vol.1, No.1, 1999, pp.44-51.
20. Falangola M.F., Jensen J.H., Babb J.S. et al., Age-related non-Gaussian diffusion patterns in the prefrontal brain, Journal of Magnetic Resonance Imaging: JMRI, Vol.28, No.6, 2008, pp.1345-1350.
21. Kang X., Herron T.J., Woods D.L., Regional variation, hemispheric asymmetries and gender differences in pericortical white matter, NeuroImage, Vol.56, No.4, 2011, pp.2011-2023.
22. Latt J., Nilsson M., Wirestam R. et al., Regional values of diffusional kurtosis estimates in the healthy brain, Journal of Magnetic Resonance Imaging: JMRI, Vol.37, No.3, 2013, pp.610-618.
23. Lobel U., Sedlacik J., Gullmar D., Kaiser W.A., Reichenbach J.R., Mentzel H.J., Diffusion tensor imaging: the normal evolution of ADC, RA, FA, and eigenvalues studied in multiple anatomical regions of the brain, Neuroradiology, Vol.51, No.4, 2009, pp.253-263.
24. Maximov I.I., Grinberg F., Shah N.J., Robust tensor estimation in diffusion tensor imaging, J. Magn. Reson., Vol.213, No.1, 2011, pp.136-144.
25. Maximov I.I., Thonnessen H., Konrad K., Amort L., Neuner I., Shah N.J., Statistical Instability of TBSS Analysis Based on DTI Fitting Algorithm, J. Neuroimaging, Vol.25, No.6, 2015, pp.883-891.
26. Alexiou G.A., Zikou A., Tsiouris S. et al., Correlation of diffusion tensor, dynamic susceptibility contrast MRI and (99m)Tc-Tetrofosmin brain SPECT with tumour grade and Ki-67 immunohistochemistry in glioma, Clinical Neurology and Neurosurgery, 116, 2014, pp.41-45.
27. Beppu T., Inoue T., Shibata Y. et al.,() Measurement of fractional anisotropy using diffusion tensor MRI in supratentorial astrocytic tumors, Journal of Neuro-Oncology, Vol.63, No.2, 2003, pp.109-116.

28. Guo A.C., Cummings T.J., Dash R.C., Provenzale J.M., Lymphomas and high-grade astrocytomas: comparison of water diffusibility and histologic characteristics, Radiology, Vol.224, No.1, 2002, pp.177-183.
29. Higano S., Yun X., Kumabe T. et al., Malignant astrocytic tumors: clinical importance of apparent diffusion coefficient in prediction of grade and prognosis, Radiology, Vol.241, No.3, 2006, pp.839-846.
30. Hilario A., Ramos A, Perez-Nunez A. et al., The added value of apparent diffusion coefficient to cerebral blood volume in the preoperative grading of diffuse gliomas, AJNR American Journal of Neuroradiology, Vol.33, No.4, 2012, pp.701-707.
31. Inoue T., Ogasawara K., Beppu T., Ogawa A., Kabasawa H., Diffusion tensor imaging for preoperative evaluation of tumor grade in gliomas, Clinical Neurology and Neurosurgery, Vol.107, No.3, 2005, pp.174-180.
32. Kang Y., Choi S.H., Kim Y.J. et al., Gliomas: Histogram analysis of apparent diffusion coefficient maps with standard- or high-b-value diffusion-weighted MR imaging--correlation with tumor grade, Radiology, Vol.261, No.3, 2011, pp.882-890.
33. Kinoshita M., Hashimoto N., Goto T. et al., Fractional anisotropy and tumor cell density of the tumor core show positive correlation in diffusion tensor magnetic resonance imaging of malignant brain tumors, NeuroImage, Vol.43, No.1, 2008, pp.29-35.
34. Kono K., Inoue Y., Nakayama K. et al.,The role of diffusion-weighted imaging in patients with brain tumors, AJNR American Journal of Neuroradiology, Vol.22, No.6, 2001, pp.1081-1088.
35. Lee E.J., Lee S.K., Agid R., Bae J.M., Keller A., Terbrugge K., Preoperative grading of presumptive low-grade astrocytomas on MR imaging: diagnostic value of minimum apparent diffusion coefficient, AJNR American Journal of Neuroradiology, Vol.29, No.10, 2008, pp.1872-1877.
36. Liu X., Tian W., Kolar B. et al., MR diffusion tensor and perfusion-weighted imaging in preoperative grading of supratentorial nonenhancing gliomas, Neuro-Oncology, Vol.13, No.4, 2011, pp.447-455.
37. Lu S., Ahn D., Johnson G., Law M., Zagzag D., Grossman R.I., Diffusion-tensor MR imaging of intracranial neoplasia and associated peritumoral edema: introduction of the tumor infiltration index, Radiology, Vol.232, No.1, 2004, pp.221-228.
38. Ma L., Song Z.J., Differentiation between low-grade and high-grade glioma using combined diffusion tensor imaging metrics, Clinical Neurology and Neurosurgery, Vol.115, No.12, 2013, pp.2489-2495.
39. Server A., Graff B.A., Josefsen R. et al., Analysis of diffusion tensor imaging metrics for gliomas grading at 3T, European Journal of Radiology, Vol.83, No,3, 2014, e156-165.
40. White M.L., Zhang Y., Yu F., Jaffar Kazmi S.A., Diffusion tensor MR imaging of cerebral gliomas: evaluating fractional anisotropy characteristics, AJNR American Journal of Neuroradiology, Vol.32, No.2, 2011, pp.374-381.

41. Wieshmann U.C., Clark C.A., Symms M.R., Franconi F., Barker G.J., Shorvon S.D., Reduced anisotropy of water diffusion in structural cerebral abnormalities demonstrated with diffusion tensor imaging, Magnetic Resonance Imaging, Vol.17, No.9, 1999, pp.1269-1274.
42. Yuan W., Holland S.K., Jones B.V., Crone K., Mangano F.T., Characterization of abnormal diffusion properties of supratentorial brain tumors: a preliminary diffusion tensor imaging study, Journal of Neurosurgery Pediatrics, Vol.1, No.4, 2008, pp.263-269.
43. Zimmerman R.D., Is there a role for diffusion-weighted imaging in patients with brain tumors or is the "bloom off the rose"? AJNR American Journal of Neuroradiology, Vol.22, No.6, 2001, pp.1013-1014.
44. Budde M.D., Xie M., Cross A.H., Song S.K., Axial diffusivity is the primary correlate of axonal injury in the experimental autoimmune encephalomyelitis spinal cord: a quantitative pixelwise analysis, The Journal of Neuroscience: the Official Journal of the Society for Neuroscience, Vol.29, No.9, 2009, pp.2805-2813.
45. Hui E.S., Cheung M.M., Qi L., Wu E.X., Towards better MR characterization of neural tissues using directional diffusion kurtosis analysis, NeuroImage, Vol.42, No.1, 2008, pp.122-134.
46. Poot D.H., den Dekker A.J., Achten E., Verhoye M., Sijbers J., Optimal experimental design for diffusion kurtosis imaging, IEEE Transactions on Medical Imaging, Vol.29, No.3, 2010, pp.819-829.
47. Veraart J., Poot D.H., Van Hecke W. et al., More accurate estimation of diffusion tensor parameters using diffusion Kurtosis imaging. Magnetic Resonance in Medicine: Official Journal of the Society of Magnetic Resonance in Medicine / Society of Magnetic Resonance in Medicine Vol.65, No.1, 2011, pp.138-145.
48. Veraart J., Van Hecke W., Sijbers J., Constrained maximum likelihood estimation of the diffusion kurtosis tensor using a Rician noise model, Magnetic Resonance in Medicine: Official Journal of the Society of Magnetic Resonance in Medicine / Society of Magnetic Resonance in Medicine, Vol.66, No.3, 2011, pp.678-686.